Electron bombardment enhancement of the reactivity of graphite with atomic hydrogen: Thresholdlike effects

D. K. Brice and C. I. H. Ashby

Citation: The Journal of Chemical Physics **81**, 6244 (1984); doi: 10.1063/1.447580
View online: http://dx.doi.org/10.1063/1.447580
View Table of Contents: http://scitation.aip.org/content/aip/journal/jcp/81/12?ver=pdfcov
Published by the AIP Publishing

Electron bombardment enhancement of the reactivity of graphite with atomic hydrogen: Threshold-like effects[a)]

D. K. Brice and C. I. H. Ashby
Sandia National Laboratories, Albuquerque, New Mexico 87185

(Received 6 April 1984; accepted 7 August 1984)

The chemical reactivity of graphite surfaces exposed to atomic hydrogen is enhanced under electron bombardment by an enhancement factor ϵ' which depends on the incident electron energy. A sharp threshold-like increase in ϵ' is observed for crystalline graphite at an energy E_{th} which depends on the angle of incidence θ of the electron beam with respect to the basal-plane surface normal. Measurements of the dependence of E_{th} on θ are reported here. Model calculations indicate that the effect is due either to a direct excitation of the electronic transition responsible for the enhancement or to plasmon production which subsequently drives the transition. Further experiments are suggested to distinguish between these mechanisms.

Electron bombardment of graphite (C) surfaces simultaneously exposed to atomic hydrogen (H) enhances the chemical reaction rate between the H and C by as much as an order of magnitude.[1-3] The origin of the enhanced reactivity is believed to be the creation of a more reactive excited state species by the excitation of the 4.8 eV π-valence to π-conduction transition[4,5] in graphite.[2] The enhanced reactivity is characterized by an enhancement factor ϵ', defined as the ratio of the increase in methane production (mol/s) to the electron current (el/s) on the reacting graphite surface. The enhancement factor ϵ' is a function of the primary electron energy E and for polycrystalline graphites $\epsilon'(E)$ correlates well with the secondary electron yield $\delta(E)$ (Fig. 1). The enhancement is thus viewed as a two step process in which the primary electrons excite secondary electrons which subsequently drive the π-band transition.

For a basal plane surface on crystalline graphite a sharp increase in ϵ' is observed at an energy E_{th}, which depends on the angle of incidence θ of the electron beam with respect to the surface normal. We report here the first measurements of the dependence of E_{th} on θ (Fig. 2) along with model calculations for several possible mechanisms for the observed threshold-like increase in ϵ'. The mechanisms considered include (i) direct excitation of the π-valence to π-conduction transition; (ii) production of surface or bulk plasmons; and (iii) excitation of surface resonance states. Mechanisms (ii) and (iii) are assumed subsequently to lead to the transition of mechanism (i). The results of these calculations suggest that the responsible mechanism is either direct excitation or the intermediate production of plasmons associated with the π-valence electron gas. Further experiments are proposed to distinguish between these alternatives.

EXPERIMENTAL

The experiments reported herein were performed in a Hg diffusion pumped glass vacuum system with base pressure of 1×10^{-8} Torr after a bake of several hours at 550 K following sample insertion. The sample studied was a graphite pseudomonocrystal of $1.2\pm0.2°$ mosaic spread (Le Carbonne–Lorraine) which was 1 mm thick and 1.4 cm in diameter. The exposed surface coincided with the hcp basal plane. Atomic H was produced from H_2 at a hot W filament. Typical H_2 pressures employed were $1.5\pm0.2\times10^{-6}$ Torr. Atomic H pressures were approximately 1/10 H_2 pressures as determined by the decrease in the $m/e=2$ quadrupole mass spectrometer (QMS) signal when the W filament was heated.[6] All experiments were performed near 300 K. Methane production was measured by the $m/e=15$ signal from the QMS, which is characteristic of methane and relatively free from interferences from the residual gases present in the system. The sample was mounted on a rotary feedthrough which was calibrated in 2° increments. The angular dependence of electron-induced effects were studied for a range of angles from 10° to $32.5°\pm1°$ off normal incidence of the primary electron beam on the graphite basal plane surface. Both positive and negative angles were employed to verify the symmetry of electron induced effects about normal inci-

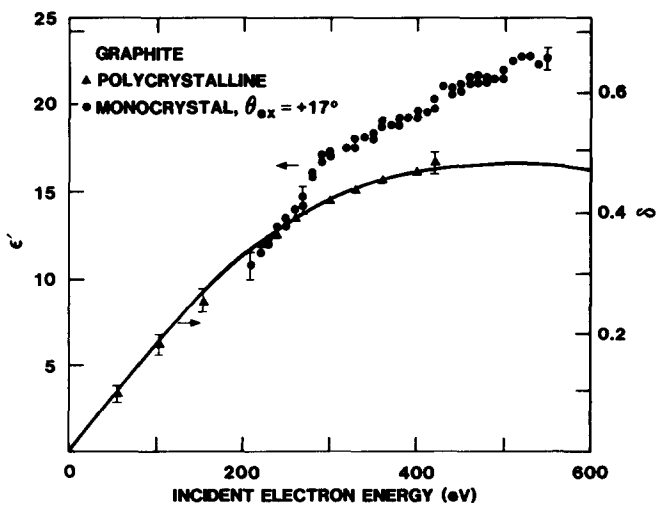

FIG. 1. Experimental electron bombardment induced methane production enhancement factor ϵ' vs primary electron energy for polycrystalline (triangles) and monocrystalline (circles) graphite. The solid line is the experimental secondary electron yield with values indicated on the right-hand ordinate.

[a)]This work performed at Sandia National Laboratories supported by the U. S. Department of Energy under contract #DE-AC04-76DP00789.

 0021-9606/84/246244-05$02.10

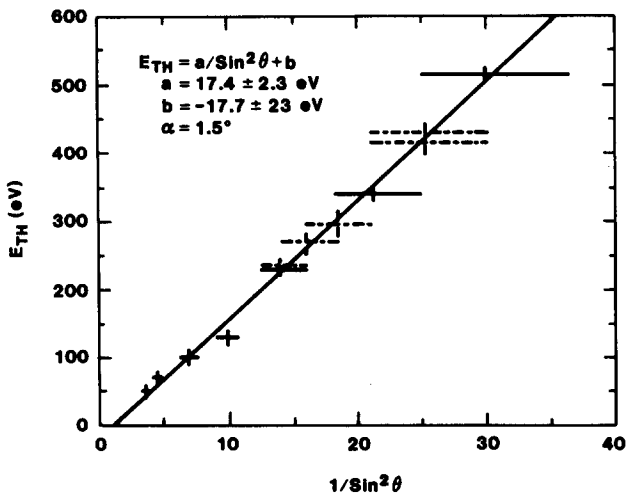

FIG. 2. Experimental values of E_{th} vs $1/\sin^2\theta$ for both positive (solid crosses) and negative (dashed crosses) angles of incidence. The straight line corresponds to a least-mean-square-error fit to the linear equation in the legend, with $\theta = \theta_{ex} - \alpha$.

dence and to calibrate the magnitude of the angular offset α of the rotary feedthrough angular indicator. The angular range studied was limited by the energy output range of the electron gun employed (40–550 V). The primary electron energy was swept from high energy to low energy in 10 V increments. The increase in CH_4 was measured by the CH_3 QMS signal at a constant current to sample. For energies greater than 200 V, a current of 10 μA was employed. Background thermal reaction production of methane was measured in the absence of electron bombardment between each energy decrement to insure that background shifts would not obscure electron induced effects.

Figure 1 shows typical experimental results for an incident angle $\theta_{ex} = 17°$, where θ_{ex} is the measured angle of incidence. A sharp increase in ϵ' is clearly seen at a primary energy of approximately 270 eV for the monocrystalline sample. Similar measurements were carried out at 12 different angles, both positive and negative angles being employed. Experimental values of $E_{th}(\theta)$ are plotted in Fig. 2 vs $1/\sin^2\theta$, where $\theta = \theta_{ex} - \alpha$. The value of α was adjusted until the plotted points for the positive (solid crosses) and negative (dashed crosses) angles fell approximately on the same curve. A least-mean-square-error (LMS) fit of the resultant $E_{th}(\theta)$ values to the function $a/\sin^2\theta + b$ was then performed and the magnitude of the LMS error noted. The procedure was iterated with different α values until the LMS error was minimized. This minimum error fit is shown in Fig. 2 as the straight line, where $a = 17.4 \pm 2.3$ eV, $b = -17.7 \pm 23.0$ eV, and $\alpha = 1.5°$. One can have confidence in this fitting procedure since small variations in α cause the plotted points for the negative and positive angles to move horizontally in opposite directions on the plot by substantial amounts. Departures from linearity are also noted for moderate changes in the value of α. The angular offset of the normal for a rotation axis perpendicular to the experimental axis of rotation was not measured. Since such offset would be added to the measured angles in quadrature its effect is of second order for the range of experimental angles used. We estimate that neglect of this effect introduces an uncertainty of less than 0.2° to our values for θ.

THEORETICAL

Simple model calculations will be presented in this section along with qualitative discussion for several possible mechanisms which could explain the observed threshold-like effect. More detailed theoretical calculations are not justified at this time since, as will be seen, sufficient uncertainty exists in our understanding of the basic processes involved to preclude a definitive identification of the source of the effect. Additional experimental measurements are proposed in the following section to distinguish among the possible mechanisms identified here.

The experimental results of Fig. 2 indicate that the threshold for the sudden increase in ϵ' is reached when the energy associated with the motion of the incident electron *parallel* to the graphite surface reaches a critical value E_c ($= a$). This suggests that the excitation involved in the effect is one which is confined to the surface basal plane, which in turn is consistent with the highly anisotropic binding of graphite.[4,5,7]

For a single particle excitation (either electron or plasmon) conservation of energy and momentum require that

$$E\cos^2\phi = (\Delta E + E_K)^2/(4E_K), \tag{1}$$

where ΔE is the energy transfer and $\hbar\mathbf{K}$ is the momentum transfer in the excitation, $E_K = \hbar^2K^2/2m$ with m the incident electron mass, and ϕ is the angle between the incident electron wave vector $\mathbf{k}$ and the excitation wave vector $\mathbf{K}$. In deriving Eq. (1) the incident electron has been assumed to have sufficient energy in both its initial and final state to be described with a free particle plane wave eigenfunction. For $\mathbf{K}$ parallel to the graphite surface and coplanar with both the surface normal and $\mathbf{k}$ Eq. (1) can be rewritten as

$$E\sin^2\theta = E_c(\Delta E, E_K), \tag{2}$$

where $E_c(\Delta E, E_K)$ is given by the right-hand side of Eq. (1).

For a fixed angle of incidence θ, Eq. (2) predicts that a given transition $(\Delta E, E_K)$ will have a threshold which corresponds to the energy for which Eq. (2) is satisfied. In order for a particular transition $(\Delta E, E_K)$ to result in the dramatic increase observed in ϵ' (Fig. 1) the transition must represent the onset for excitations of a given type, or the probability for the particular transition must be large compared with the corresponding probability for transitions with slightly less energy.

The Brillouin zone (BZ) of graphite has two hexagonal faces with normal parallel to the c axis and six equivalent rectangular faces with normal perpendicular to the c axis. The π-band transition which has been identified as the origin of the enhanced methane production[2] occurs at the point Q in the BZ, i.e., at the center of one of the rectangular faces. The transition is identified as the $Q_{2g}^- $ to Q_{2u}^- transition at 4.8 eV. The calculated band structure of graphite shows π bands which are relatively flat near the point Q and thus the joint density of states for vertical ($K = 0$) interband transitions exhibits a large peak[4,5,7] for energies near 4.8 eV. Both experimental[8–10] and theoretical[8] determinations of the joint

density of states for nonvertical interband transitions ($K \neq 0$) show that for **K** perpendicular to the c axis the peak near 4.8 eV remains a prominent feature for K values as large as 0.3–0.4 K_Q, where K_Q is the magnitude of the BZ vector at the point Q. For larger K values the peak no longer appears in the joint density of states. It is further observed that the peak energy also increases by ~ 1 eV[10] as the value of K increases from zero up to the value at which the peak in the joint density of states disappears.

If one identifies the disappearance of the peak in the joint density of states as the threshold for direct excitation of the transition responsible for the enhanced methane production, Eqs. (1) and (2) then yield $E_c \sim 5$–10 eV. However, because of the energy shift which occurs as K is increased the threshold may occur at a somewhat lower value for K. That is, the peak energy shift may move the peak away from the particular transition which drives the enhanced methane production. Since E_c is a decreasing function of E_K when E_K is less than ΔE, a smaller value of K leads to a larger value for E_c. Accepting the experimental value for E_c (17.4 eV) and ΔE (4.8 eV), one obtains from Eqs. (1) and (2) $E_K \simeq 0.4$ eV, or $K \simeq 0.22\ K_Q$. This value for K is reasonably near the cutoff value discussed in the previous paragraph. Although this discussion has been semiquantitative it is nevertheless evident that the experimental results of Fig. 2 are reasonably consistent with the onset of direct excitation of the 4.8 eV π-band transition through the Coulomb interaction of the incident electron with the crystal electrons.

For single plasmon excitation, ΔE in the expression on the right-hand side of Eq. (1) is replaced by the plasmon energy $\hbar\omega_K$, and **K** becomes the excited plasmon wave vector. Equation (2) also holds for plasmon excitation providing similar restrictions are placed on **K**. Bulk plasmons are restricted to **K** vectors parallel to the graphite surface here since methane production occurs at the graphite surface. Plasmons with other **K** vectors would carry the excitation energy away from the surface and thus are less likely to influence the surface reactivity.

Graphite exhibits two independent modes of collective electron oscillation, one mode consisting of oscillations of the $(\sigma + \pi)$ electrons and the other oscillations of the π electrons alone.[11,12] Experimental dispersion relations are available only for the bulk π plasmons in graphite.[8,12] As a result we have used theoretical expressions for the dispersion relations for both the surface[13] and bulk[14] plasmons in calculating the minimum value for E_c from Eqs. (1) and (2). The experimental dispersion relations were also used to calculate E_c for the bulk π plasmons in order to provide a "realistic" value for E_c, and in order to be able to estimate the uncertainty associated with the theoretical results. The resultant E_c values are collected in Table I, along with wavelengths of the plasmons associated with the threshold ($\lambda = 2\pi/K$). The range of E_c values in the table obtained from the experimental dispersion relations reflects a slight anisotropy of ω_K as a function of the azimuthal angle of **K** about the c axis.

The tabulated values for E_c for plasmon excitation in the π valence electron gas are reasonably consistent with the measured value of E_c from the results plotted in Fig. 2. Furthermore, the very short plasmon wavelengths are such that

TABLE I. Values of E_c calculated for the plasmon production threshold. λ is the plasmon wavelength at threshold.

Plasmon type	E_c(eV)	λ (Å)
Surface plasmons		
π oscillation	13.5	7.1
$(\sigma + \pi)$ oscillation	>31	<3.1
Bulk plasmons with K parallel to surface		
π oscillations	15.8[a]	7.0[a]
	11.5–13.5[b]	~ 5.4[b]
$(\sigma + \pi)$ oscillation	49	3.2

[a] From theoretical ω_K.
[b] From experimental ω_K.

rapid decay of these plasmons through the production of electron-hole pairs is expected. We thus feel that π-plasmon excitation is a reasonable candidate mechanism for the source of the threshold-like effect observed in Fig. 1. Plasmon excitation in the $(\sigma + \pi)$-valence electron gas would seem to be ruled out as the origin of the threshold-like effect, since the calculated values for E_c are significantly larger than the measured value.

It has been proposed that swift charged particles may create plasmon shock waves by their passage through materials, and that these shock waves decay through single electron excitations (Mach electrons).[15] Although some limited experimental evidence suggests Mach electron production,[16] the existence of such excitations has yet to be confirmed and theoretical considerations have been advanced indicating that such plasmon shock waves cannot be produced.[14] These shock waves, if they exist, are thought to be related to a resonance in the cross section for single particle excitation by a swift charged particle.[17] Since the excitation of such shock waves can also account for the observed angular dependence of E_{th}, providing the shock waves travel parallel to the graphite surface, we have calculated the expected values for E_c for this mechanism. From Eqs. (3.10) and (5.2) of Ref. 17 one obtains $E_c(\pi) = 14.3$ eV and $E_c(\sigma + \pi) = 32.5$ eV, where the shock waves are produced in the π and $(\sigma + \pi)$ plasmons, respectively. These values are near the corresponding values obtained for single plasmon production, and this mechanism could thus be considered roughly as simply another form of plasmon excitation.

A final mechanism considered for the threshold-like effect of Figs. 1 and 2 is the capture of the incident electron into surface resonance states.[18] These states form a continuum which can be characterized by a reciprocal surface net vector **G**, and a wave vector **K** which lies in the first Brillouin zone of the surface (i.e., a two-dimensional zone). Threshold-like effects in exciting these states can occur at a zone boundary crossing. Thus, with **K** lying on the zone boundary E_c can be determined from conservation of parallel momentum yielding

$$E_c(\text{surface resonance}) = \hbar^2|\mathbf{K} + \mathbf{G}|^2/2m. \tag{4}$$

Calculated values of E_c for surface resonance states in graphite yield $E_c(G = 0) \leqslant 11.1$ eV and $E_c(G \neq 0) > 44$ eV. Thus, the excitation of surface resonance states by the incident electrons is inconsistent with the measured value of E_c.

TABLE II. Calculated values of E_c for incident protons. Also, values for E_{th} at $\theta = 30°$.

Mechanism	E_c(keV)	E_{th} 30° (keV)
Surface π plasmons	9.2	37
Bulk π plasmons with K parallel to surface	11.6	47
Direct excitation of 4.8 eV π band transition	27.4	110

DISCUSSION

The semiquantitative model calculations of the previous section lead to the following view of the processes associated with the enhanced methane production due to electron bombardment of graphite under atomic hydrogen attack. For energies less than E_{th} the primary electron loses energy by exciting secondary electrons to states far removed from the 4.8 eV π-band transition responsible for the enhanced methane production.[2] These secondary electrons and their associated collision cascades of tertiary, etc., electrons subsequently excite the 4.8 eV transition to some degree leading to an enhancement factor which is proportional to the secondary electron production (Fig. 1). When the primary energy rises to E_{th} a new mechanism for exciting the 4.8 eV transition is activated; either a direct excitation of the transition by the primary electron, or the onset of π-plasmon production in the surface layer with subsequent plasmon decay thereby exciting the transition.

We remark that both the experimental[10] and theoretical[8] electron energy loss functions show losses to bulk π plasmons which are an order of magnitude larger than the losses to direct excitation at 4.8 eV. Further, the width of the plasmon loss peak[8,9] ($\sim$1–2 eV) indicates that these plasmons quickly decay ($\tau \sim 10^{-14}$–10^{-15} s) providing an efficient mechanism for electron-hole pair excitation. This leads us to favor π-plasmon production as the mechanism leading to the threshold-like effect observed in the enhanced methane production. We should caution, however, that direct excitation can not be ruled out as the underlying mechanism since the electron energy loss function gives no direct information on the efficiency with which the plasmons subsequently excite the 4.8 eV π-band transition.

More detailed theoretical calculations are beyond the scope of the present investigation. It is our view, however, that such calculations would be unable to distinguish between the two mechanisms which are favored by the model calculations which have been carried out here and by the available experimental data. Indeed, such additional calculations would be complicated by the fact that the details of the process(es) whereby the 4.8 eV π-band transition drives the enhanced methane production have yet to be worked out.

Although additional theoretical calculations appear unlikely to resolve the choice between the two favored mechanisms, further experimental measurement utilizing atomic projectile bombardment shows promise of providing the necessary evidence for the selection of one of these mechanisms. For projectiles other than electrons it is only necessary to replace the electron mass m in the definition of E_K with the projectile mass in order that the expressions of Eqs. (1) and (2) remain valid. We have used the measured value of E_c for the incident electrons (Fig. 2) to calculate the corresponding expected value of E_c for incident protons for both the direct excitation and π-plasmon production mechanisms. These results are listed in Table II. For the direct excitation the calculation assumed that ΔE and K remained the same for the heavier projectiles. For the plasmon excitations the plasmon dispersion relations were adjusted to give agreement between calculation and experiment for incident electrons and these altered dispersion relations were used to calculate the proton values for E_c. Also collected in Table II are calculated values of E_{th} for protons incident at 30° with respect to the surface normal. Note that the values in Table II are in keV while those of Table I are in eV.

A different value of E_c for incident protons results for each of the three different mechanisms considered. While the differences are not sufficiently great to distinguish between the two plasmon modes, direct excitation is clearly distinct from plasmon excitation. Similar calculations can be easily carried out for other atomic projectiles. In fact, for these heavier projectiles the value of E_c is very nearly proportional to the particle mass so that relatively accurate values can be obtained from the results in Table II by simply multiplying by the atomic mass number. While it is known that bombardment of graphite by energetic hydrogen results in methane production,[19] systematic studies of the enhancement of methane production as a function of projectile energy have not been made, nor have studies utilizing crystalline graphite been carried out.

Finally, the mechanisms considered here for the threshold-like increases in methane production under electron bombardment do not require single crystal graphite for their operation. Thus, similar results should be expected for polycrystalline material. However, because of the dramatic onset of these effects and their strong angular dependence, such effects may be obscured in the polycrystalline material because of its mosaic spread. This may account for the lack of observation of the effects in polycrystalline material, although systematic measurements have not been made.

SUMMARY AND CONCLUSIONS

A sharp increase in the electron bombardment enhanced chemical reactivity of graphite with atomic hydrogen is observed at an incident electron energy E_{th}. The first measurements of the dependence of E_{th} on the electron angle of incidence θ are reported here. The results are such that $E_{th} \times \sin^2 \theta = \text{constant}$.

In order to identify the origin of the threshold-like increase in the enhancement, model calculations are presented for several mechanisms. From these calculations we conclude that the active mechanism is either direct excitation of the 4.8 eV π-band transition at the point Q in the Brillouin zone, or production of π plasmons which subsequently decay, at least part of the time, through excitation of the 4.8 eV transition. If this latter mechanism proves to be the relevant

process it is, to our knowledge, the first time that plasmons have been implicated, even indirectly, in surface chemical reactions.

Finally, experiments are proposed which show promise of being able to distinguish between the two mechanisms above. These experiments involve observation of the threshold-like increases in enhanced reactivity due to atomic projectile bombardment. Model calculations are presented which show that for incident protons the threshold-like increase occurs at distinctly different energies for the two different mechanisms. Similar results are expected for other atomic projectiles.

[1]C. I. H. Ashby and R. R. Rye, J. Nucl. Mater. **92**, 141 (1980).
[2]C. I. H. Ashby, Appl. Phys. Lett. **43**, 609 (1983).
[3]O. Auciello, A. A. Haasz, P. C. Strangeby, and P. R. Underhill, *Proceedings of the 9th Symposium on Engineering Problems of Fusion Research, Oct. 26–29, 1981,* IEEE Publ. No. 81CH1715-2NPS, p. 252.
[4]D. L. Greenaway, G. Harbeke, F. Bassani, and E. Tosatti, Phys. Rev. **178**, 1340 (1969).
[5]F. Bassani and G. Pastori Parravicini, Nuovo Cimento B **50**, 95 (1967).
[6]R. K. Gould, J. Chem. Phys. **51**, 541 (1979).
[7]P. R. Wallace, Phys. Rev. **71**, 622 (1947).
[8]K. Zeppenfeld, Opt. Commun. **1**, 119 (1969); Z. Phys. **243**, 229 (1971).
[9]H. Venghaus, Phys. Status Solidi B **66**, 175 (1974).
[10]U. Büchner, Phys. Status Solidi B **81**, 227 (1977).
[11]K. Zeppenfeld, Thesis, Hamburg, 1969; H. Venghaus, Phys. Status Solidi B **71**, 609 (1975).
[12]H. Raether, *Excitation of Plasmons and Interband Transitions by Electrons* (Springer, New York, 1980).
[13]D. E. Beck, Phys. Rev. B **4**, 1555 (1971).
[14]R. H. Ritchie, Phys. Rev. **106**, 874; (1957); Nucl. Instrum. Methods **198**, 81 (1982).
[15]J. F. Hoffman, H. Stocker, W. Scheid, W. Greiner, V. Ceausescu, and E. Badralxe, Z. Phys. A **280**, 131 (1977); W. Schafer, H. Stocker, B. Muller, and W. Greiner, *ibid.* **288**, 349 (1978); Z. Phys. B **36**, 319 (1980).
[16]H. J. Frischkorn, K. O. Groenveld, S. Schumann, R. Latz, G. Reichhardt, J. Schader, W. Kronast, and R. Mann, Phys. Lett. A **76**, 155 (1980).
[17]D. K. Brice and P. Sigmund, Dan. Vid. Selsk. Mat. Fys. Medd. **40**, No. 8 (1980).
[18]See, for example, the review article by E. G. McRae, Rev. Mod. Phys. **51**, 541 (1979).
[19]See, for example, J. Roth, J. Bohdansky, and K. L. Wilson, J. Nucl. Mater. **111/112**, 775 (1982).